ChemComm

Accepted Manuscript

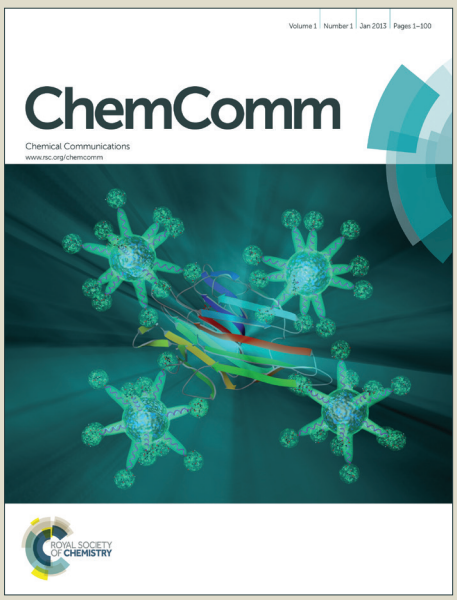

ROYAL SOCIETY OF CHEMISTRY

www.rsc.org/chemcomm

Journal Name

RSCPublishing

COMMUNICATION

One-pot synthesized DNA-templated Ag/Pt bimetallic nanoclusters as peroxidase mimics for colorimetric detection of thrombin

Cite this: DOI: 10.1039/xOxxOOOOOx

Received OOth January 2012,
Accepted OOth January 2012

DOI: 10.1039/xOxxOOOOOx

www.rsc.org/

Cheng Zheng,[a] Ai-Xian Zheng,[a] Bo Liu,[a] Xiao-Long Zhang,[a] Yu He,*[a] Juan Li,[a] Huang-Hao Yang*[a] and Guonan Chen[a]

We developed a facile one-step approach to synthesize DNA-templated Ag/Pt bimetallic nanoclusters (DNA-Ag/Pt NCs), which possess highly-efficient peroxidase-like catalytic activity. With this finding, an aptamer based sandwich-type strategy is employed to design a label-free colorimetric aptasensor for the protein detection with high sensitivity and selectivity.

Rapid advances in nanotechnology have opened a new door for the development of nanomaterials in the biocatalysis field.[1] Nowadays, peroxidase-like or oxidase-like activities have been discovered in various types of nanomaterials, such as metal oxide nanomaterials,[2] carbon nanomaterials,[3] and noble-metal nanoparticles (NPs).[4] As low-cost alternatives to natural enzymes, these nanomaterial-based enzyme mimics, termed nanozymes,[1b] hold significant advantages including good stability, tunable enzymatic activities, and design flexibility. Currently, composite nanomaterials including bimetallic NPs[5] and hybrid nanomaterials[6] have emerged as promising nanozymes and attracted much attention due to their highly improved catalytic performance. This is mainly benefited from the synergistic effect and/or electronic effect of the individual components.[7]

Up to now, nanozyme-based bioassays have been readily applied to the sensing of DNA and protein.[4a,7b,8,9] In these colorimetric aptasensors or immunosensors, nanozymes are usually required to conjugate with recognition moieties such as antibodies and DNA probes.[9] However, the conjugation of nanozymes with biomolecules could cause the loss of the binding affinity of biomolecules[7b,10] and also the decrease of the catalytic efficiency of nanozymes.[2c,4a] In addition, it is difficult to functionalize small-size NPs with biomolecules, such as nanoclusters (NCs).[11]

In recent years, DNA has been renowned for its capacity to act as building block for *in situ* fabrication of functional materials, including DNA nanoscaffold,[12] metallic nanowires,[13a] quantum dots,[13b] and metal NPs/NCs.[14] These DNA-templated nanomaterials exhibit outstanding properties of facile synthesis, precisely controlled size, and excellent biocompatibility. More importantly, there is no requirement of additional functionalization of DNA-templated nanomaterials with biomolecules for the biosensor construction. Although many works have been done to explore DNA-templated Ag NCs and DNA-templated Au NCs as fluorescent probes,[15] their application in enzyme mimic catalysis are rarely reported due to their poor catalytic properties. Most recently, Pt nanomaterials are found to be a highly effective peroxidase mimics.[4b,16] Chen *et al* prepared a peroxidase-mimicking DNA-Pt complex from ssDNA to establish a colorimetric bioassay of thrombin.[17] Unfortunately, preparation process of DNA-Pt complex was relatively complicated and time-consuming. Moreover, since the growth of Pt NPs was random on the DNA, it was inevitable for Pt NPs to generate on the aptamer, which may lead to the loss of binding ability of aptamer and thus the reduction of sensitivity or selectivity during the sensing.

In this work, we developed a facile one-step approach to produce Ag/Pt bimetallic nanoclusters through a DNA-templated method. The obtained DNA-templated Ag/Pt bimetallic nanoclusters (DNA-Ag/Pt NCs) display peroxidase-like catalytic activity and can catalyze hydrogen peroxide (H_2O_2)-mediated oxidation of substrate, 3,3,5,5-tetramethylbenzidine (TMB), to produce a blue color reaction (Fig. 1A). We choose a pre-selected C-rich DNA (template DNA in Table S1, ESI†) as synthesis template, which has been utilized to template the formation of fluorescent Ag NCs. Because the cytosine bases exhibit strong affinity for Ag(I),

Ag(I) could preferentially interact with C-rich DNA and form Ag NCs after reduced with $NaBH_4$. Then Pt(0) growth would be initiated by the galvanic replacement reaction between Ag(0) and Pt(II) on the surface of Ag NCs and continue by the reduction with $NaBH_4$. Since encapsulated in DNA matrix, the growth of the deposited Pt NCs would be well controlled on a few nanometer scale. In contrast to previous studies,[16-18] no additional surfactant or high temperature was needed in our synthesis.

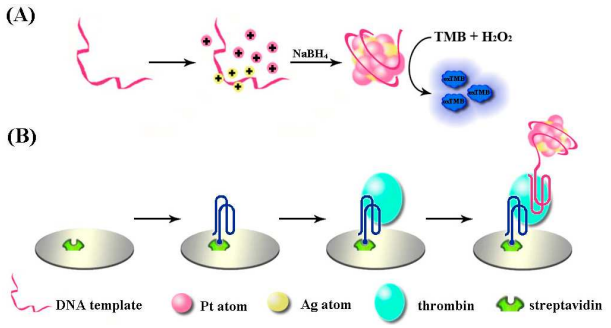

Fig. 1 Schematic illustration of (A) DNA-Ag/Pt NCs synthesis protocol and (B) colorimetric detection of human thrombin based on DNA-Ag/Pt NCs.

The size distribution of the as-synthesized DNA-Ag/Pt NCs was characterized with transmission electron microscopy (TEM). The DNA-Ag/Pt NCs, with average diameter of about 2.11 nm, are well dispersed and roughly spherical (Fig. 2A and 2B). The small particle size might be attributed to the stabilization provided by DNA template. Different from brightly fluorescent DNA-Ag NCs, nearly complete fluorescence quenching was observed for DNA-Ag/Pt NCs (Fig. 2C). It suggested that Pt NCs were deposited on the Ag NCs surface, since quenching efficiency is dependent upon the separation distance.[19] A typical Energy-dispersive X-ray (EDX) spectrum of DNA-Ag/Pt NCs is given in Fig. 2D, where elemental Ag and Pt are clearly detected, indicating the successful formation of Ag/Pt bimetallic NCs. The X-ray spectroscopy (XPS) analysis reveals the presence of the peaks for Pt $4f_{7/2}$ at 71.09 eV and for Ag $3d_{5/2}$ at 367.63 eV, respectively (Fig. S1, ESI†).

The peroxidase-like catalytic activity of DNA-Ag/Pt NCs was studied in the catalysis of TMB oxidation with H_2O_2. As illustrated in Fig. 3A, the absorbance intensity at 652 nm, which is the characteristic peak of oxidized TMB, greatly increased within 10 min when DNA-Ag/Pt NCs were added (curve c).The phenomenon indicates the intrinsic peroxidase-like activity of DNA-Ag/Pt NCs. However, DNA-Ag NCs showed negligible catalytic activity (curve b). We inferred that the peroxidase-like activity of DNA-Ag/Pt NCs was mainly attributed to Pt NCs that were deposited onto the Ag NCs. In this synthesis, Ag NCs are speculated to act as a support for the Pt NCs deposition. To confirm our hypothesis, the identical preparation procedure but without the addition of $AgNO_3$ was carried out. No obvious catalytic reaction occurred in this system (curve b in Fig. S2, ESI†), indicating that Pt NCs could not be formed in the absence of Ag NCs under our synthesis condition. The reason is presumed that the affinity of nucleobases towards Pt ions is much weaker than that towards Ag ions. Furthermore, DNA-Ag/Pt NCs also could not be synthesized by C-poor DNA template (random DNA and Apt15 in Table S1, as well as curve c and d in Fig. S2, ESI†), highlighting that a C-rich DNA template is crucial to the formation of Ag/Pt NCs.

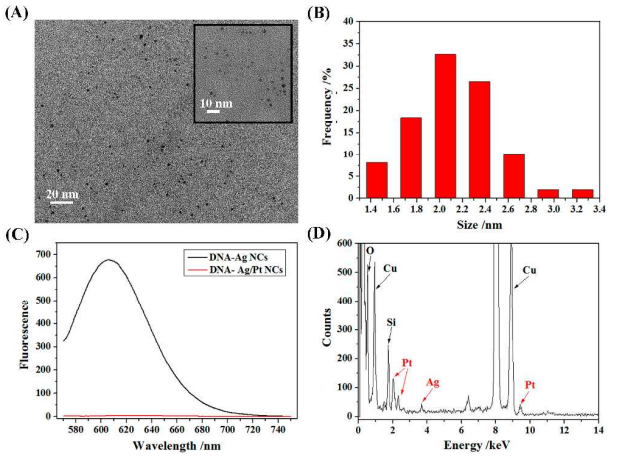

Fig. 2 (A) TEM images of DNA-Ag/Pt NCs. Inset: the magnified TEM image. (B) Histogram of the particle size distribution of DNA-Ag/Pt NCs. (C) Fluorescence spectra of DNA-Ag NCs and DNA-Ag/Pt NCs obtained at an excitation of 548 nm. (D) EDX spectrum of DNA-Ag/Pt NCs.

To further evaluate the catalytic activity of DNA-Ag/Pt NCs, we prepared a DNA-Pt complex according to the synthesis method reported by Chen *et al*.[17] As shown in Fig. 3B, DNA-Ag/Pt NCs exhibit much higher peroxidase-like activity than that of DNA-Pt complex at equivalent dose of Pt content. We attribute the higher catalytic activity of DNA-Ag/Pt NCs to two features. First, DNA-Ag/Pt NCs have a much smaller size than that of DNA-Pt complex (tens of nanometers). For the nanozymes with similar composition and surface properties, smaller sized ones often exhibit higher activity.[1b,2a] Second, DNA-Ag/Pt NCs are composed of Ag and Pt. The electronic charge transfer effect and the synergistic effect among Ag and Pt could promote the adsorption and the efficient oxidation of reactants, thereby offering an improved catalytic activity.[20] Moreover, some reports have confirmed that Ag in bimetallic NPs can enhance the catalytic activities or optical responses of the other alloying metal.[21] Based on the discussion above, it can be concluded that Ag NCs play an important role for both the clusters formation and the enhanced catalysis.

For the purpose to get high catalytic activity, the preparation conditions of DNA-Ag/Pt NCs, including K_2PtCl_4 and $AgNO_3$ concentrations as well as the preparation time, have been optimized. Fig. S3 (ESI†) reveals that the optimal concentration ratio of K_2PtCl_4:$AgNO_3$ was 2:1, and the optimum preparation time was chosen as 3 h. DNA-Ag/Pt NCs display highest catalytic activity in the acetate buffer of pH 4 and the H_2O_2 concentration of 50 mM (Fig. S4, ESI†). Compared with horseradish peroxidase (HRP), the catalytic activity of DNA-Ag/Pt NCs remained stable in the wide pH and temperature

range (Fig. S5, ESI†). It indicates that DNA-Ag/Pt NCs could serve as a promising platform for design and development of the nanozyme-mediated colorimetric assays.

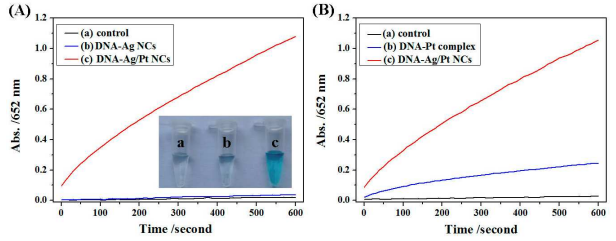

Fig. 3 (A) The time-dependent absorbance changes of the systems containing (a) H_2O_2 + TMB; (b) DNA-Ag NCs + H_2O_2 + TMB; (c) DNA-Ag/Pt NCs + H_2O_2 + TMB in 200 mM acetate buffer (pH 4.0). Inset: photograph of different catalytic systems. (B) Catalytic reactions of (b) DNA-Pt complex and (c) DNA-Ag/Pt NCs in the TMB-H_2O_2 system as a function of time.

In order to explore the practical application of DNA-Ag/Pt NCs, we developed a colorimetric sensing platform for the detection of protein (Fig. 1B). We employed human thrombin as a model target protein. In this assay, a biotinylated 29-mer thrombin aptamer was introduced to the streptavidin-coated 96-well microplates through biotin-streptavidin interaction. A ssDNA (template-Apt15 in Table S1, ESI†) containing template DNA and 15-mer thrombin aptamer was used as template agent to synthesize aptamer-functionalized Ag/Pt NCs. When target thrombin was present, the specific binding of the two aptamers to target resulted in a thrombin-Ag/Pt NCs complex, which was immobilized on the plates. Then the bound DNA-Ag/Pt NCs, as signal detection probe, catalyzed the oxidation of TMB to produce colorimetric signals, which provide a quantitative determination of human thrombin.

Followed the conventional ELISA procedure, H_2SO_4 was used to stop the catalytic reaction in which the oxidized TMB was further oxidized to a yellow diimine with a maximum absorption wavelength of 452 nm (Fig. S6, ESI†). So we recorded the absorbance intensity at 452 nm to quantify the thrombin. There was a visually observable color change correlated to thrombin concentrations (Fig. 4A). Meanwhile, in the UV-vis spectra, the absorbance at 452 nm increased as human thrombin concentration increased (Fig. 4B). Furthermore, the absorption intensity was linear to the concentrations of human thrombin in the range from 1 nM to 50 nM (Fig. 4C), with a calibration function of A=0.0192C + 0.0679 (R^2=0.995). The detection limit was calculated to be 2.6 nM (defined as 3σ, where σ is the standard deviation of the blank). The detection limit was much lower than that of the colorimetric assay based on DNA-Pt complex (400 nM).[17] We presume that this improved sensitivity is due to the higher catalytic activity of DNA-Ag/Pt NCs and the efficient retention of recognition property of aptamer. In this study, the pre-selected DNA template is a specific sequence for the synthesis of DNA-Ag/Pt NCs. Besides that, it has been proved above that Ag/Pt NCs could not grow on the Apt15. Therefore, the recognition function of aptamer to thrombin would be not affected.

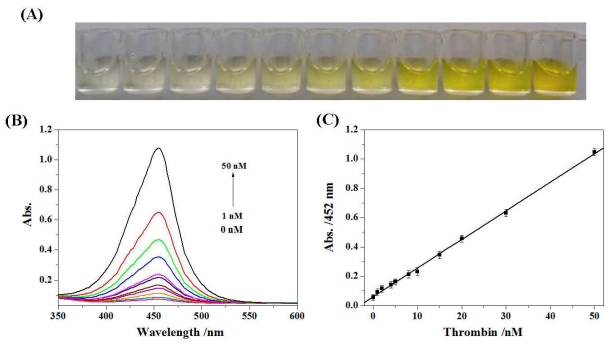

Fig. 4 (A) Photograph and (B) absorption spectra of the system after incubation with different concentrations of human thrombin (0, 1, 2, 4, 5, 8, 10, 15, 20, 30, 50 nM). (C) The absorption intensity at 452 nm was plotted as a function of the concentrations of human thrombin.

The selectivity of the proposed aptasensor described herein was determined in Fig. S7 (ESI†). Obviously, the system displayed a significant change in the absorbance intensity in the presence of human thrombin. Nevertheless, negligible detectable signals were obtained towards the other proteins. Furthermore, we applied this colorimetric aptasensor to detect human thrombin in human serum samples. 10-fold diluted human serum samples were spiked with different amounts of human thrombin. As listed in Table S2 (ESI†), it can be seen that the thrombin analysis in diluted human serum samples showed good recovery.

In summary, the DNA-Ag/Pt NCs have been successfully prepared through a facile DNA-templated method in a mild reaction condition. We prove that a C-rich DNA template has an essential role for the clusters formation. The obtained DNA-Ag/Pt NCs show intrinsic peroxidase-mimicking activity. their high catalytic performance could be attributed to their ultrasmall size and the synergistic effect among the alloying metals. Based on this, we developed a label-free colorimetric aptasensor for the detection of target thrombin, allowing a detection limit of 2.6 nM. For this aptasensor, the template DNA sequence for the clusters is directly coupled with a thrombin aptamer. This design strategy can not only avoid chemical conjugation of Ag/Pt NCs with aptamer, but also preserve the affinity and specificity of aptamer to its target. The proposed aptasensor is capable of detecting target in complicated biological samples such as human serum. Furthermore, it can be easily expanded to the determination of other targets by preparing DNA-Ag/Pt NCs containing other target-specific aptamers. Taken together, our work would provide a novel and general strategy to design nanozyme-mediated colorimetric assays for the DNA/protein detection. We expected that it would hold potential applications in biomedical diagnosis, environmental monitoring, and therapeutics.

This work was supported by the National Basic Research Program of China (No. 2010CB732403), the National Natural Science Foundation of China (No. 21125524), the Program for Changjiang Scholars and Innovative Research Team in

University (No. IRT1116) and the National Science Foundation of Fujian Province (No. 2010J06003).

Notes and references

[a] The Key Lab of Analysis and Detection Technology for Food Safety of the MOE, Fujian Provincial Key Laboratory of Analysis and Detection Technology for Food Safety, College of Chemistry and Chemical Engineering, Fuzhou University, Fuzhou 350002, People's Republic of China.
E-mail: hhyang@fio.org.cn, heyu@fzu.edu.cn.

† Electronic Supplementary Information (ESI) available: experimental details and additional figures. See DOI: 10.1039/c000000x/

1 (a) Y, Song, W. Wei and X. Qu, *Adv. Mater.*, 2011, **23**, 4215-4236. (b) H. Wei and E. Wang, *Chem. Soc. Rev.*, 2013, **42**, 6060-6093. (c) Y. Lin, J. Ren and X. Qu, *Acc. Chem. Res.*, 2014, **47**, 1097-1105.

2 (a) L. Gao, J. Zhuang, L. Nie, J. Zhang, Y. Zhang, N. Gu, T. Wang, J. Feng, D. Yang, S. Perrett and X. Yan, *Nat. Nanotechnol.*, 2007, **2**, 577-583. (b) J. Mu, Y. Wang, M. Zhao and L. Zhang, *Chem. Commun.*, 2012, **48**, 2540-2542. (c) A. Asati, S. Santra, C. Kaittanis, S. Nath and J. M. Perez, *Angew. Chem. Int. Ed.*, 2009, **48**, 2308-2312.

3 (a) A.-X. Zheng, Z.-X. Cong, J.-R. Wang, J. Li, H.-H. Yang and G.-N. Chen, *Biosens. Bioelectron.*, 2013, **49**, 519-524. (b) J. Tian, Q. Liu, A. M. Asiri, A. H. Qusti, A. O. Al-Youbi and X. Sun, *Nanoscale*, 2013, **5**, 11604-11609.

4 (a) X. Zheng, Q. Liu, C. Jing, Y. Li, D. Li, W. Luo, Y. Wen, Y. He, Q. Huang, Y.-T. Long and C. Fan, *Angew. Chem. Int. Ed.*, 2011, **50**, 11994-11998. (b) J. Fan, J.-J. Yin, B. Ning, X. Wu, Y. Hu, M. Ferrari, G. J. Anderson, J. Wei, Y. Zhao and G. Nie, *Biomaterials*, 2011, **32**, 1611-1618. (c) M. Stobiecka, *Biosens. Bioelectron.*, 2014, **55**, 379-385.

5 (a) S. Ge, F. Liu, W. Liu, M. Yan, X. Song and J. Yu, *Chem. Commun.*, 2014, **50**, 475-477. (b) C.-I. Wang, W.-T. Chen and H.-T. Chang, *Anal. Chem.*, 2012, **84**, 9706-9712. (c) W. He, Y. Liu, J. Yuan, J.-J. Yin, X. Wu, X. Hu, K. Zhang, J. Liu, C. Chen, Y. Ji and Y. Guo, *Biomaterials*, 2011, **32**, 1139-1147.

6 (a) L.-N. Zhang, H.-H. Deng, F.-L. Lin, X.-W. Xu, S.-H. Weng, A.-L. Liu, X.-H. Lin, X.-H. Xia and W. Chen, *Anal. Chem.*, 2014, **86**, 2711-2718. (b) X. Chen, G. Wu, J. Chen, X. Chen, Z. Xie and X. Wang, *J. Am. Chem. Soc.*, 2011, **133**, 3693-3695. (c) J. W. Lee, H. J. Jeon, H.-J. Shin and J. K. Kang, *Chem. Commun.*, 2012, **48**, 422-424.

7 (a) M. Chen, D. Kumar, C.-W. Yi and D. W. Goodman, *Science*, 2005, **310**, 291-293. (b) M. Liu, H. Zhao, S. Chen, H. Yu and X. Quan, *ACS Nano*, 2012, **6**, 3142-3151.

8 C.-W. Lien, C.-C. Huang and H.-T. Chang, *Chem. Commun.*, 2012, **48**, 7952-7954.

9 (a) Q. Wang, J. Lei, S. Deng, L. Zhang and H. Ju, *Chem. Commun.*, 2013, **49**, 916-918. (b) Z. Tang, H. Wu, Y. Zhang, Z. Li and Y. Lin, *Anal. Chem.*, 2011, **83**, 8611-8616. (c) R. Thiramanas, K. Jangpatarapongsa, P. Tangboriboonrat and D. Polpanich, *Anal. Chem.*, 2013, **85**, 5996-6002.

10 S. H. D. P. Lacerda, J. J. Park, C. Meuse, D. Pristinski, M. L. Becker, A. Karim and J. F. Douglas, *ACS Nano*, 2010, **4**, 365-379.

11 N. Ma, G. Tikhomirov and S. O. Kelley, *Acc. Chem. Res.*, 2010, **43**, 173-180.

12 (a) R. Hu, X. Zhang, Z. Zhao, G. Zhu, T. Chen, T. Fu and W.Tan, *Angew. Chem. Int. Ed.*, 2014, **53**, 5821-5826. (b) G. Zhu, J. Zheng, E. Song, M. Donovan, K. Zhang, C. Liu and W. Tan, *Proc. Natl. Acad. Sci. USA*, 2013, **110**, 7998-8003.

13 (a) C. F. Monson and A. T. Woolley, *Nano Letters*, 2003, **3**, 359-363. (b) C. Zhang, X. Ji, Y. Zhang, G. Zhou, X. Ke, H. Wang, P. Tinnefeld and Z. He, *Anal. Chem.*, 2013, **85**, 5843-5849.

14 (a) Z. Qing, X. He, D. He, K. Wang, F. Xu, T. Qing and X. Yang, *Angew. Chem. Int. Ed.*, 2013, **52**, 9719-9722. (b) H. Liu, X. Zhang, X. Wu, L. Jiang, C. Burda and J.-J. Zhu, *Chem. Commun.*, 2011, **47**, 4237-4239.

15 (a) S. Choi, R. M. Dickson and J. Yu, *Chem. Soc. Rev.*, 2012, **41**, 1867-1891. (b) T. A. C. Kennedy, J. L. MacLean and J. Liu, *Chem. Commun.*, 2012, **48**, 6845-6847.

16 Z. Gao, M. Xu, L. Hou, G. Chen and D. Tang, *Anal. Chim. Acta*, 2013, **776**, 79-86.

17 A. Higuchi, Y.-D. Siao, S.-T. Yang, P.-V. Hsieh, H. Fukushima, Y. Chang, R.-C. Ruaan and W.-Y. Chen, *Anal. Chem.*, 2008, **80**, 6580-6586.

18 H. You, Z. Peng, J. Wu and H. Yang, *Chem. Commun.*, 2011, **47**, 12595-12597.

19 J. M. Slocik, A. O. Govorov and R. R. Naik, *Angew. Chem. Int. Ed.*, 2008, **47**, 5335-5339.

20 (a) R. Ferrando, J. Jellinek and R. L. Johnston, *Chem. Rev.*, 2008, **108**, 845-910. (b) H. Zhang and N. Toshima, *Catal. Sci. Technol.*, 2013, **3**, 268-278.

21 W. He, X. Wu, J. Liu, X. Hu, K. Zhang, S. Hou, W. Zhou and S. Xie, *Chem. Mater.*, 2010, **22**, 2988-2994.

